

Cover Page



Universiteit Leiden



The handle <http://hdl.handle.net/1887/22623> holds various files of this Leiden University dissertation

**Author:** Boom, Maria Catharina Anna

**Title:** Opioid therapy : a trade-off between opioid-analgesia and opioid-induced respiratory depression

**Issue Date:** 2013-12-03

CHAPTER 4  
UTILITY FUNCTION:  
A RISK-BENEFIT COMPOSITE OF PAIN RELIEF AND  
BREATHING RESPONSES

---

M.C.A. Boom MD, Erik Olofsen MSc, Meike Neukirchen PhD, René Fussen Dr  
me, MD, Justin Hay PhD, Geert Jan Groeneveld MD PhD, Leon Aarts MD PhD,  
Elise Sarton MD PhD, ALbert Dahan MD PhD

(After revision published in) *Anesthesiology*. 2013 Sep;119(3):663-74

## 4.1 INTRODUCTION

It is well known that opioids are able to produce life-threatening respiratory depression.<sup>1</sup> A recent editorial brought to attention the sharp rise, since the early 1990s, of unintentional drug overdose and consequently loss of life due to ingestion of prescription painkillers in the United States.<sup>2</sup> As discussed, this is related to a 10-fold increase in the medical use of synthetic opioids, marketing tactics and the proactive identification of patients with chronic pain.<sup>2</sup> Also in the perioperative setting opioid-induced respiratory depression is a common observation with regular reports of fatalities.<sup>3-5</sup> Overall there is the ongoing need for vigilance when potent opioids are administered to spontaneously breathing and opioid-naïve patients.<sup>1,2</sup> Opioid risk (in the acute setting: respiratory depression) is best viewed in context of its beneficial effect, ie. analgesia. Recently, Katz proposed the construction of a risk benefit composite for opioid use in chronic pain patients. This composite is based on days of chronic pain treatment causing pain relief  $\geq 30\%$  and no or mild adverse effects.<sup>1</sup> One method to quantify opioid-induced respiratory depression relative to analgesia is the construction of a Utility (or safety) Function (UF). Cullberg first introduced the concept of UFs when characterizing the outcome of a thrombin inhibitor.<sup>6</sup> He defined the UF as the probability of drug-induced thrombus regression minus the probability of drug-induced bleeding related event. In the current study we constructed the UF for the opioid analgesic fentanyl. The fentanyl UF is constructed based on the results of a population pharmacokinetic-pharmacodynamic (PK-PD) study on the effect of fentanyl on respiration and antinociception. Next, a simulation study is performed, using the PK-PD parameter estimates and their variances, in which 9,999 simulated subjects received fentanyl. The resultant distributions are used to calculate the UF. In the current approach we calculated the probability of an increase in pain tolerance of 50% or more minus the probability of respiratory depression of 50% or more.

## 4.2 METHODS EN MATERIALS

### 4.2.1 SUBJECTS

After approval of the protocol by the local Human Ethics Committee (Commissie Medische Ethiek, LUMC, Leiden) and the Central Committee on Research involving Human Subjects (Commissie Mensgebonden Onderzoek, The Hague, The Netherlands) and informed consent was obtained according to the Declaration of Helsinki, 12 male volunteers, aged 18-45 years, were initially recruited to participate in the study. One subject dropped out and was replaced by a 13th subject. All recruits were subjected to a medical history, physical examination, 12-leads electrocardiogram and blood screening before inclusion. Only healthy subjects, without a history of alcohol or illicit drug abuse and a body mass index between 20 and 28, were included in the study.

#### 4.2.2 STUDY DESIGN

All subjects were studied twice with at least two weeks between sessions (the sequence of sessions was random). On one occasion the effect of a single intravenous infusion of fentanyl ( $3.5 \mu\text{g}\cdot\text{kg}^{-1}$  infusion over 90-s) on respiration was tested, on the other occasion the effects of fentanyl ( $3.5 \mu\text{g}\cdot\text{kg}^{-1}$  infusion over 90-s) pain responses to a cutaneous noxious electrical stimulus were tested.

**Respiratory measurements.** During the respiratory studies, subjects breathed through a facemask (fitted over nose and mouth). The airway gas flow was measured with a pneumotachograph (#4813, Hans Rudolph, Kansas City, MO) connected to a pressure transducer, which yielded a volume signal. The pneumotachograph was heated ( $37^\circ\text{C}$ ) throughout the study period. This signal was calibrated with a 1 L calibration syringe (Hans Rudolph). The pneumotachograph was connected to a T-piece; one arm of the T-piece received a gas mixture with a flow of  $45 \text{ L}\cdot\text{min}^{-1}$  from a gas mixing system, consisting of three mass-flow controllers (Bronkhorst High-Tec, Veenendaal, The Netherlands) via which the flow oxygen, nitrogen and carbon dioxide could be set individually at any desired level. A computer provided control signals to the mass-flow controllers allowing adjustment of the inspired gas mixture to force the end-tidal gas concentrations of oxygen and carbon dioxide to follow a specific pattern in time. Gas concentrations were measured with a gas analyzer (Datex Multicap, Helsinki, Finland); arterial hemoglobin oxygen saturation was measured via a finger probe with a Masimo pulse oximeter (Irvine, CA). Respiration was measured at a clamped elevated end-tidal carbon dioxide tension ( $\text{PCO}_2$ ) using the 'Dynamic End-Tidal Forcing' (DEF) technique.<sup>7-10</sup> In each subject, the end-tidal  $\text{PCO}_2$  was elevated in steps of 2-3 mmHg until ventilation reached a value 20 -  $24 \text{ L}\cdot\text{min}^{-1}$ . The end-tidal  $\text{PCO}_2$  was kept constant at this level throughout the study (baseline end-tidal  $\text{PCO}_2$  level). This procedure was performed in a 'training' session 30 to 45 min prior to dosing. The end-tidal oxygen concentration ( $\text{PO}_2$ ) was kept constant at 110 mmHg throughout the study. After a steady state in ventilation was obtained, fentanyl was infused and continuous breath-to-breath ventilatory measurements were obtained for the next 90 min. Thereafter, 3-min measurements were obtained at 30-min intervals until  $t = 4$  h following administration and at 1-h intervals until  $t = 6$  h. The following variables were collected on a breath-to-breath basis on a computer disc for further analysis: inspiratory minute ventilation, end-tidal  $\text{PCO}_2$ , end-tidal  $\text{PO}_2$  and oxygen saturation.

**Pain responses.** Acute pain was induced by an electrical current through two surface electrodes (Red Dot, 3M, London, Ontario, Canada) placed on the skin overlaying the left tibial bone (transcutaneous electrical stimulation).<sup>10-12</sup> The electrodes were attached to a computer interfaced current stimulation (Leiden University Medical Center, Leiden, The Netherlands). The intensity of the noxious stimulation was increased from 0 mA in steps of  $0.5 \text{ mA}\cdot 2 \text{ s}^{-1}$ . The stimulus train consisted of a square-wave pulse of 0.2 ms duration

applied at 10 Hz and had a cutoff of 128 mA. The subjects were instructed to press a control button when they felt pain (pain threshold) and when no further increase in stimulus intensity was acceptable (pain tolerance; this ends the stimulus train). Pain responses were obtained at baseline and at  $t = 10, 25, 40, 55, 70, 90, 110, 130, 160, 190, 220, 250, 310$  and  $370$  min. after dosing. We analyzed the pain tolerance data for the current report.

**Blood sampling and plasma drug concentrations measurements.** Blood samples (3 mL) were obtained from an arterial line placed in the left or right radial artery (opposite of the arm through which the drug was infused) for determination of the plasma concentrations of fentanyl. Blood samples were obtained at  $t = 2, 5, 10, 15, 30, 60, 90, 150, 210, 270, 330, 390$  and  $480$  min after dosing. Plasma was separated within 30 min of blood collection and stored at  $-20^{\circ}\text{C}$  until analysis.

Samples were prepared by liquid/liquid extraction of the plasma samples with *t*-butyl methyl ether. Samples with fentanyl concentrations above the calibration range were diluted prior to the measurement using human blank plasma. Chromatographic separation was performed using an Agilent 1200 liquid chromatograph (Agilent Technologies Inc., Santa Clara, CA) and a PAL HTC-xt (Axel Semrau GmbH & Co., Sprockhövel, Germany) autosampler. A Pursuit  $3\mu$  C18  $30 \times 2$  (30 mm  $\times$  2 mm) column (Varian, Walnut Creek, CA) and MetaGuard Pursuit  $3\mu$  C18  $10 \times 2$  mm guard column (Varian, Walnut Creek, CA) were used as stationary phases. The analytes were eluted using gradient elution with a mobile phase consisting of formic acid (0.1%) and acetornitril (containing 0.1% formic acid) at  $30^{\circ}\text{C}$  with a flow rate of  $0.7 \text{ ml}\cdot\text{min}^{-1}$ . Fentanyl was detected in the MRM mode using an electrospray ion source on a triple quadrupole mass spectrometer API-5500 QTrap equipped with a Turbo-Ionspray™ Interface (Applied Biosystems, Framingham, MA) operating in positive ionization mode. The MS/MS transitions 337/188 for fentanyl and 342/188 for D5-fentanyl were monitored for quantitation of the compound. The calibration range of the bioanalytical assay was  $0.005 - 5.00 \text{ ng}\cdot\text{ml}^{-1}$ . Calibration samples were prepared at 0.005, 0.010, 0.050, 0.200, 1.00, 2.00, 3.75 and  $5.00 \text{ ng fentanyl}\cdot\text{mL}^{-1}$  plasma. Quality control samples were prepared at concentrations of 0.015, 2.00 and  $5.00 \text{ ng fentanyl}\cdot\text{ml}^{-1}$  plasma. The values for the overall accuracy and the overall precision for quality controls assayed during analysis of study samples were 97.2% – 106.2% and 1.7% – 9.5%, respectively. The samples were analyzed in six batches with interbatches accuracy of 95.9% – 104.9% and coefficient of variation of 1.9 – 6.9% over the calibration range of  $0.005$  to  $5.0 \text{ ng}\cdot\text{ml}^{-1}$ .

#### 4.2.3 PHARMACOKINETIC-PHARMACODYNAMIC ANALYSIS

Multiple compartment models were fitted to the fentanyl pharmacokinetic data. Model selection (the number of compartments) was based on the Goodness of Fit criterion. Only the 'best' models will be described here.

To eliminate a possible hysteresis between plasma concentration and effect, an effect

compartment was postulated that equilibrates with the plasma compartment with a half-life  $t_{1/2}k_{e0}$  (i.e., the blood-effect-site equilibration half-life).

The ventilation data were modeled as:<sup>7-10</sup>

$$\text{Effect}(t) = E_{\text{max}} + [E_{\text{min}} - E_{\text{max}}] \cdot [A / (1+A)] \text{ and } A = [\text{Ce}(t) / C_{50}]^{\gamma} \quad \text{eqn.(1)}$$

where effect is the effect at time  $t$  (minute ventilation),  $E_{\text{max}}$  maximum or predrug effect (baseline ventilation),  $E_{\text{min}}$  minimum effect (an  $E_{\text{min}}$  of zero indicates that apnea may be reached),  $\text{Ce}(t)$  effect-site concentration at time  $t$ , and  $C_{50}$  the effect-site or steady-state concentration causing 50% depression of ventilation.

Transcutaneous electrical pain responses were modeled as:<sup>10-12</sup>

$$\text{Pain Response}(t) = \text{Baseline} \cdot [1 + 0.25 \cdot B] \text{ and } B = [\text{Ce}(t) / C_{25}]^{\gamma} \quad \text{eqn.(2)}$$

where  $\text{Pain Response}(t)$  is the stimulus intensity at which a pain tolerance response occurs at time  $t$ ,  $\text{Baseline}$  the predrug stimulus intensity at which a pain threshold or pain tolerance response occurs,  $\text{Ce}(t)$  the effect-site concentration at time  $t$ , and  $C_{25}$  the effect-site or steady-state concentration causing an increase of 25% stimulus intensity for a response. Estimation of  $C_{25}$  rather than  $C_{50}$  was performed as the 25% increase in stimulus intensity was midpoint of the observed responses.

The pharmacokinetic-pharmacodynamic data were analyzed with the mixed-effects modeling software NONMEM VII (ICON Development Solutions, Ellicott City, MD)<sup>13</sup> The PK/PD analysis was performed in two stages. From the first stage (pharmacokinetic analysis), empirical Bayesian estimates of the pharmacokinetic parameters were obtained. In the second stage (pharmacodynamic analysis), the pharmacokinetic parameters were fixed to those obtained in the first stage. An integrated data analysis was performed in NONMEM, *i.e.* combining all pharmacodynamic data (respiratory and pain data) in one analysis. Model parameters were assumed to be log-normally distributed. Residual error was assumed to have both an additive and a relative error for concentrations and only an additive error for all effect parameters. Covariance between random effects ( $\eta$ s) for the pharmacodynamic end-points were explored using \$OMEGA BLOCKS.

The number of compartments in the pharmacokinetic analysis was determined by the magnitude of the decrease in the minimum objective function value (MOFV;  $\chi^2$ -test;  $P < 0.01$  was considered significant). In the pharmacokinetic analysis weight and height were considered as covariates.  $P$ -values less than 0.01 were considered significant.

#### 4.2.4 VISUAL PREDICTIVE CHECK

Visual predictive checks were performed to assess the adequacy of the description of both fixed and random effects by simulating data using the models and calculating their 2.5<sup>th</sup>,

50<sup>th</sup> and 97.5<sup>th</sup> percentile at all sampling times.

#### 4.2.5 UTILITY FUNCTION

The utility of drug effect,  $U$ , was defined as the probability of obtaining the desired effect minus the probability of obtaining a side effect.<sup>6,14</sup> If we define the desired effect as an increase in pain tolerance of 50% or more and the side effect as respiratory depression of 50% or more, and the probability of obtaining these as  $P(A) \geq 0.5$  and  $P(R) \geq 0.5$ , respectively, then  $U = P(A \geq 0.5) - P(R \geq 0.5)$ . The utility of fentanyl's effect was calculated as function of effect site concentration ( $U_1$ ) and of time ( $U_2$ ) after administration of  $3.5 \mu\text{g}\cdot\text{kg}^{-1}$ :

$$U_1(C_e) = P(A(C_e) \geq 0.5) - P(R(C_e) \geq 0.5) \quad \text{eqn.(3)}$$

and

$$U_2(t) = P(A(t) \geq 0.5) - P(R(t) \geq 0.5) \quad \text{eqn.(4),}$$

where  $P$  is probability,  $A$  analgesia and  $R$  respiratory depression.

The UF was calculated from the population pharmacokinetic and pharmacodynamic model with established values for the population and their inter-individual variability parameters ( $\omega^2$ ). To this end  $2 \times 9,999$  simulations were performed using NONMEM's simulation step (with SUBPROBLEMS = 9999). The occurrence of desired and side effects were counted and divided by 9999 to estimate probabilities (note that these are uncorrelated because no correlations between the  $\omega^2$  were identified in the pharmacodynamic analysis).  $U$ -values range from  $-1$  to  $+1$ ;  $U > 0$  indicate that the chance for a desired effect exceeds the chance for an unwanted effect (here respiratory depression) while  $U < 0$  indicates that the chance for the unwanted effect exceeds the chance for analgesia.  $U$ -values between  $-0.2$  and  $0.2$  are small effects,  $U$ -values between  $-0.2$  and  $-0.4$ , and  $0.2$  and  $0.4$  are moderate effects and  $U$ -values  $< -0.4$  and  $> 0.4$  are large effects. Small effects indicate absence of selectivity of action (*i.e.*, no clinically relevant greater chance for analgesia than for respiratory depression and *vice versa*).

Sensitivity analyses were performed to assess the effect of changes in context (numerical response thresholds in  $P(A)$  and  $P(R)$ ) and effect of changes in pain parameter estimates  $t_{1/2k_{e0}}$  and  $C_{50}$  on the form of the utility functions.

#### 4.3 RESULTS

One subject dropped out and was replaced by another. The pharmacodynamic data of the dropout were incomplete and therefore discarded. His pharmacokinetic data were used in the population analysis. Consequently the number of subjects was 13 for the pharmacokinetic data and 12 for the pharmacodynamic data. In one subject just one set

of pharmacokinetic data was available due to failure of arterial line insertion on one occasion. No unexpected or major side effects occurred during the studies. All subjects ( $n = 13$ ) were white males with a mean age of 22.1 years (range 19-27 years), height 186 cm (176-200 cm), weight 80.5 kg (64-111 kg) and body mass index of  $23.2 \text{ kg}\cdot\text{m}^{-2}$  (21-28  $\text{kg}\cdot\text{m}^{-2}$ ).

Mean fentanyl plasma concentrations, respiration and pain responses are shown in Figure 1. In Figure 2, the individual pain responses are plotted showing the variability in the data. The peak increase in pain tolerance averaged to 21.9 mA, which (apart from one outlier of 91 mA) was normally distributed (range 5.5 to 33.5 mA,  $n = 11$ ). Similar response variabilities have been observed in other studies on opioid analgesic efficacy using this same pain model.<sup>10-12</sup>

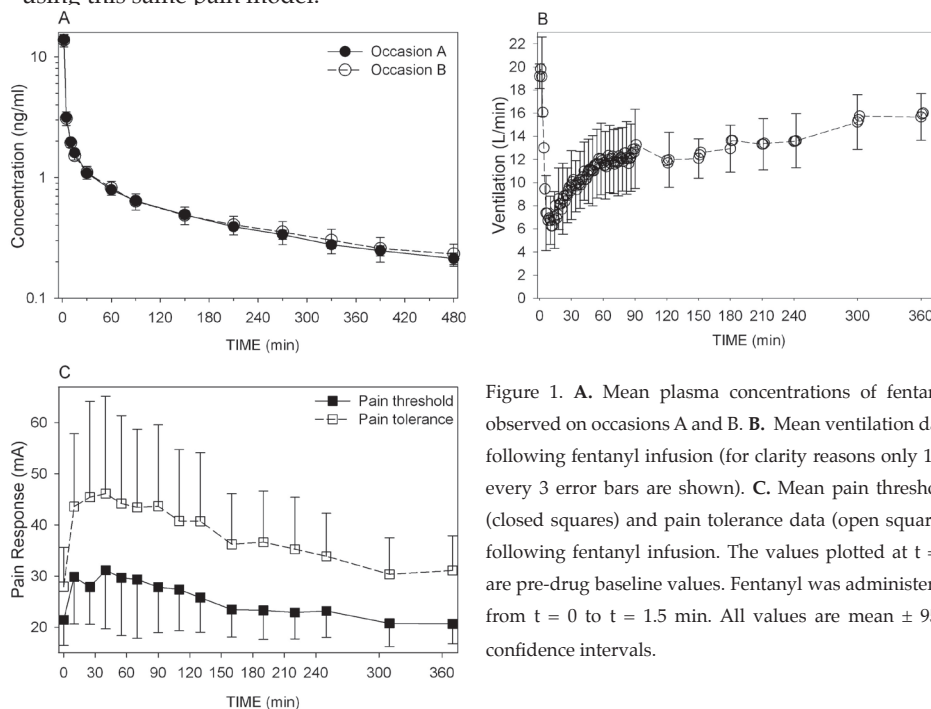
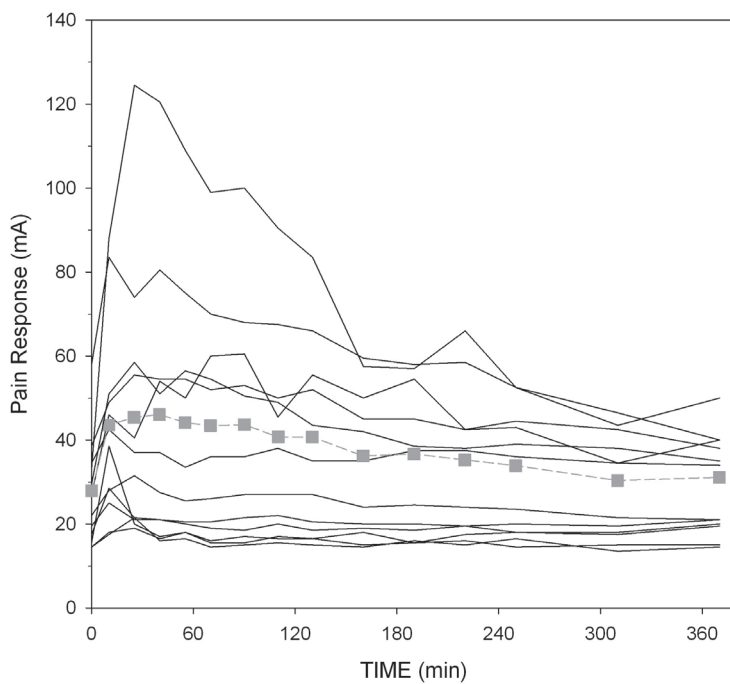


Figure 1. **A.** Mean plasma concentrations of fentanyl observed on occasions A and B. **B.** Mean ventilation data following fentanyl infusion (for clarity reasons only 1 in every 3 error bars are shown). **C.** Mean pain threshold (closed squares) and pain tolerance data (open squares) following fentanyl infusion. The values plotted at  $t = 0$  are pre-drug baseline values. Fentanyl was administered from  $t = 0$  to  $t = 1.5$  min. All values are mean  $\pm$  95% confidence intervals.

#### 4.3.1 PHARMACOKINETIC ANALYSIS

The mean plasma fentanyl concentrations are given in Figure 1A. The variability in fentanyl concentrations obtained on the two distinct study occasions was small as observed in Figure 1A. The final pharmacokinetic model consisted of a three-compartment model with one central ( $V_1$ ) and two peripheral compartments ( $V_2$  and  $V_3$ ). The pharmacokinetic





**Figure 2.** Spaghetti-plot of the pain tolerance responses during and following fentanyl infusion. The lines are the individual responses, the orange squares are the mean data.

**Table 1. Pharmacokinetic model parameter estimates**

Parameter	Typical value	SEE (%)	$\omega^2$	SEE	$\eta$ -shrinkage <sup>&amp;</sup>
$V_1$ (L)	8.867	0.652 (7)	0.065*	0.021 (32)	1%
$V_2$ (L)	42.056	3.243 (8)	0.042	0.016 (38)	4%
$V_3$ (L)	191.709	9.529 (5)	0.027	0.011 (41)	4%
$CL_1$ ( $L \cdot h^{-1}$ )	0.751	0.0538 (7)	0.027	0.016 (59)	4%
$CL_2$ ( $L \cdot h^{-1}$ )	4.291	0.322 (8)	0.065*	0.021 (32)	6%
$CL_3$ ( $L \cdot h^{-1}$ )	1.932	0.157 (8)	0.065*	0.021 (32)	6%
IOV on $CL_1$	0.004	0.002 (50)			77%
$\sigma^2$	0.109	0.005 (5)			8% <sup>#</sup>

\* one  $\eta$  was used for  $V_1$ ,  $CL_2$  and  $CL_3$ .

SEE is standard error of the estimate in the column to the left (in brackets the SEE as %).

$V_1$ ,  $V_2$  and  $V_3$  are the volumes of compartments 1, 2 and 3;  $CL_1$  is elimination clearance;  $CL_2$  and  $CL_3$  are the clearances between compartment 1 and compartment 2 and 3, respectively.

IOV is inter-occasion variability.

$\omega^2$  is the inter-subject variability (in the log-domain).

$\eta^2$  is the variance of the residual (relative) error.

&:  $\eta$  shrinkage of empirical Bayesian estimates to the population values.

#:  $\epsilon$  shrinkage of model output to the observations.

parameter estimates are given in Table 1. Covariate weight (WT in kg) had a significant effect on parameters  $V_1$ ,  $V_2$ ,  $CL_1$  and  $CL_2$  with the volumes scaled by  $(WT/70)$  and the clearances scaled by  $(WT/70)^{0.75}$  ( $P < 0.01$ ). No effect of WT was observed for  $V_3$  and  $CL_3$ . Covariate height had no effect on any of the model parameters. Goodness of fit plots (measured versus individual predicted concentrations and individual weighted residuals versus time) are given in Fig. 3. Examples of data fits are given in Figures 4 and 5. The goodness of fit plots and inspection of the individual data fits indicate that the pharmacokinetic model adequately describes the pharmacokinetic data.

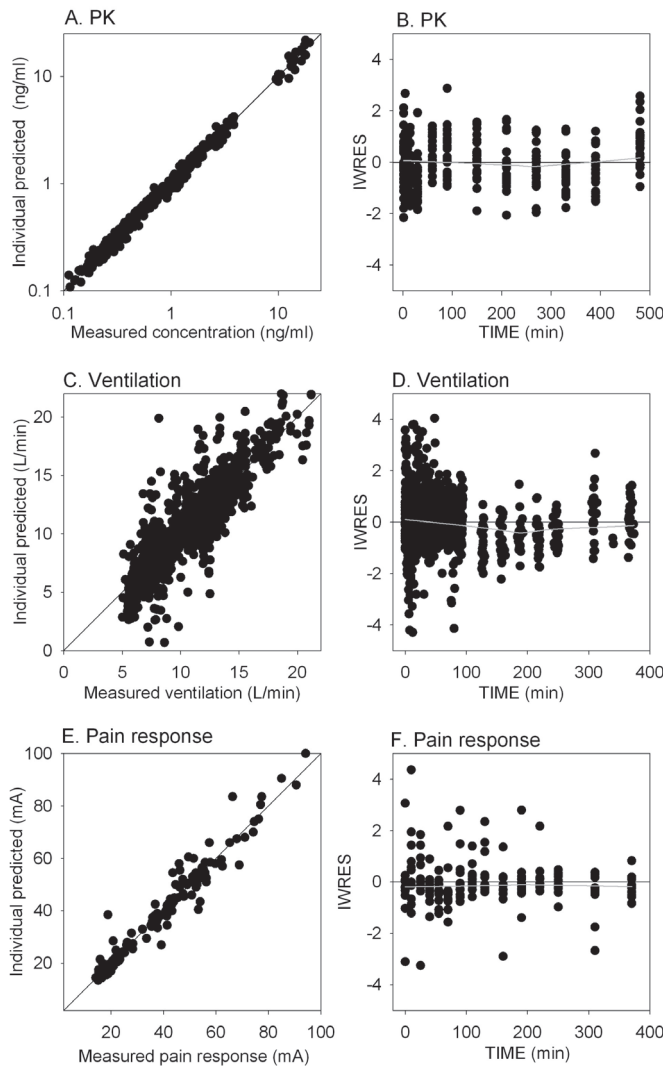


Figure 3. Goodness of fit plots.

A. Individual predicted concentrations versus measured concentration.

B. Individual weighted residual (IWRES) of concentration versus time.

C. Measured ventilation versus individual predicted ventilation.

D. Individual weighted residuals (IWRES) of ventilation versus time.

E. Measured versus individual predicted pain response.

F. IWRES of pain tolerance responses versus time. In panels B, D and F Loess smoothers are given in grey. PK is pharmacokinetics.

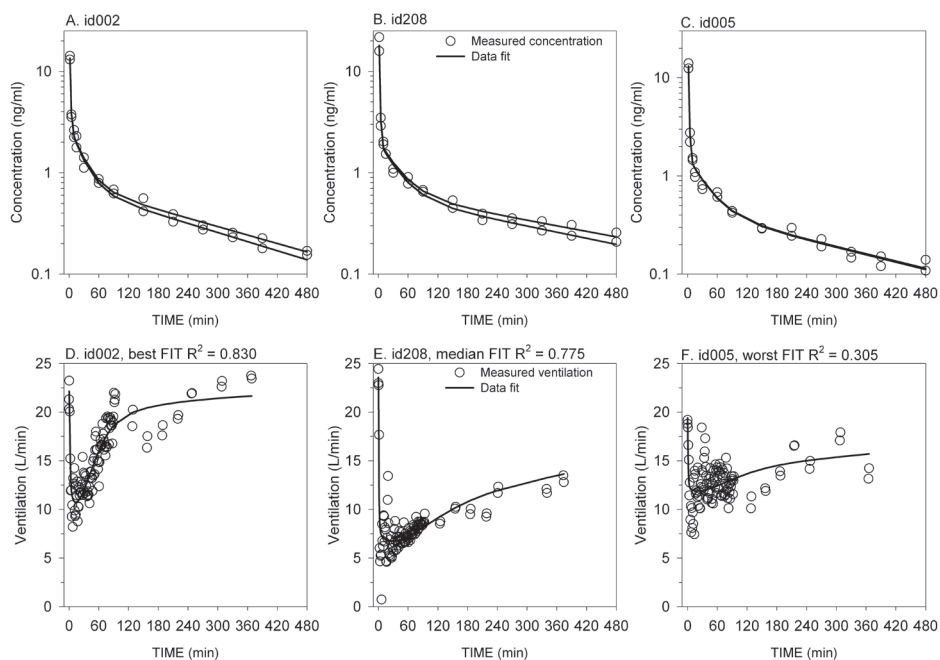


**Figure 4.** Effect of fentanyl on ventilation. Best, median and worst fits (as determined by the coefficient of determination,  $R^2$ ) are given together with the corresponding pharmacokinetic data fits. Open symbols are the measured values; the continuous lines are the data fits. **A** and **D.** subject id 002, best pharmacodynamic fit; **B** and **E.** subject id 208, median pharmacodynamic fit; **C** and **F.** subject id 005, worst pharmacodynamic fit. Since fentanyl was given on two occasions both pharmacokinetic fits are given (panels A-C).

#### 4.3.2 PHARMACODYNAMIC ANALYSIS

Mean ventilatory and pain responses are given in Figures 1 and 2. These figures show that fentanyl had an appreciable effect on both end-points. Best, median and worst PD data fits (and corresponding pharmacokinetic fits; the pharmacokinetic fits include the data from both occasions) for the three end-points are given in Fig. 4 and 5. The goodness of fit plots are given in Figure 3C to F. These plots and inspection of the individual data fits indicate that the pharmacodynamic models adequately describe the pharmacodynamic data. Model parameter values are given in Table 2. The ventilation  $E_{min}$  value was not significantly different from 0  $L \cdot min^{-1}$  ( $P > 0.05$ ), which indicates that at a sufficiently high fentanyl dose apnea will occur. A critical ventilation level (arbitrarily defined as  $< 4 L \cdot min^{-1}$  or 20% of baseline) is attained at steady-state plasma fentanyl concentrations of 4  $ng \cdot ml^{-1}$  or greater. Potency estimates for respiratory depression and pain responses were 1.0  $ng \cdot ml^{-1}$  ( $C_{50}$ ) and 0.9  $ng \cdot ml^{-1}$  ( $C_{25}$ ), respectively ( $P < 0.01$ ). The intra-individual variabilities ( $\eta$ s) were not correlated indicating that the parameter values ( $t_{1/2}k_{e0}$ ,  $C_{50}$  and  $\gamma$ ) of the three end-points were uncorrelated. Peak respiratory depression ranged among subjects from 7 to 12 min following the start of the 90-s infusion.

The results of the Visual Predictive Checks (VPC) for pharmacokinetic and pharmacodynamic data are plotted in Figure 6, showing the median predicted values (continuous lines) and 95% intervals (dashed lines).

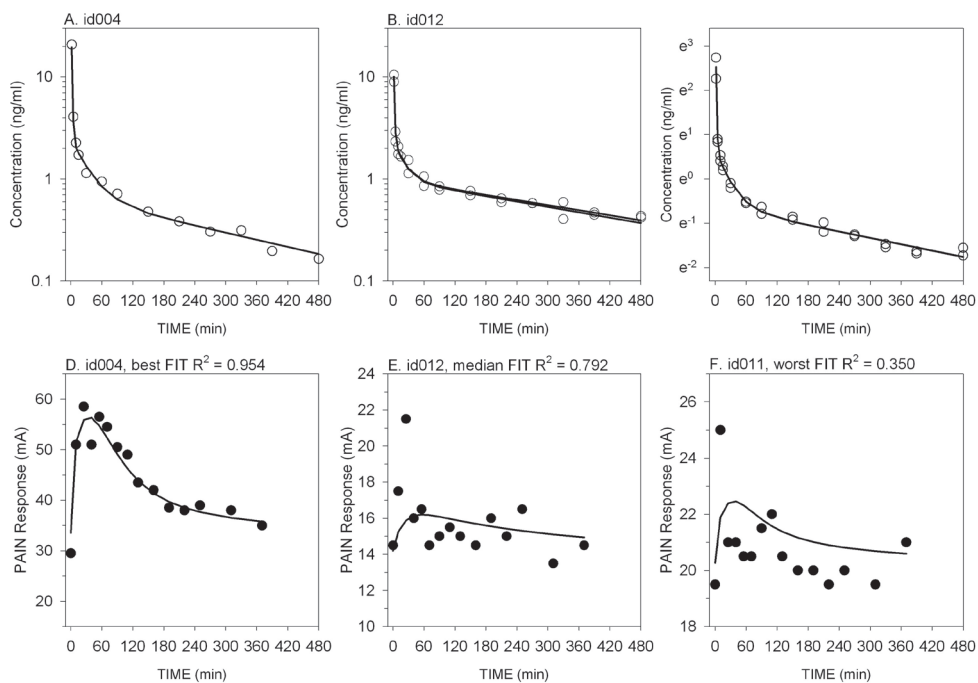


**Figure 5.** Effect of fentanyl on pain tolerance. Best, median and worst fits (as determined by the coefficient of determination,  $R^2$ ) are given, together with the corresponding pharmacokinetic data fits. **A** and **D**. subject id 004, best pharmacodynamic fit; **B** and **E**. subject id 012, median pharmacodynamic fit; **C** and **F**. subject id 011, worst pharmacodynamic fit. Since fentanyl was given on two occasions both pharmacokinetic fits are given if available (panels A-C; subject id004 has PK data from just one occasion).

Table 2. Fentanyl pharmacodynamic model parameters

	Typical value	SEE (%)	$\omega^2$	SEE	$\eta$ -shrinkage <sup>&amp;</sup>
<b>Ventilation</b>					
$t_{1/2}k_{e0}$ (min)	17.10	3.44 (20)	0.49	0.12 (24)	-2%
$E_{max}$ (L.min <sup>-1</sup> )	19.90	0.92 (5)	0.02	0.01 (50)	1%
$E_{min}$ (L.min <sup>-1</sup> )	0 (fixed)	*	0 (fixed)	*	-
$C_{50}$ (ng.ml <sup>-1</sup> )	1.02	0.18 (18)	0.31	0.07 (23)	-2%
$\gamma$	1 (fixed)	*	0.41	0.26 (63)	*
$\Sigma^2$	3.71	0.59 (16)			1% #
<b>Pain Relief Response</b>					
$t_{1/2}k_{e0}$ (min)	41.6	9.27 (22)	0.15	0.07 (47)	20%
Baseline tolerance (mA)	26.0	2.87 (7)	0.14	0.04 (29)	-5%
$C_{25}$ (ng.ml <sup>-1</sup> )	0.91	0.29 (32)	0.85	0.35 (41)	16%
$\gamma$	1.59	0.05 (3)	0 (fixed)	*	-
$\sigma^2$	10.9	3.84 (35)			8% #

\*: not estimable.

$\omega^2$  is the inter-subject variability (in the log-domain),  $\sigma^2$  is the variance of the residual error.

$t_{1/2}k_{e0}$  is the blood-effect-site equilibration constant;  $C_{50}$  and  $C_{25}$  are potency parameters or steady-state concentrations at which 50% or 25% of the effect occurred;  $E_{max}$  is baseline ventilation level;  $E_{min}$  is the minimum ventilation level;  $\gamma$  is a shape parameter.

- Not included in the statistical model.

SEE is standard error of the estimate in the column to the left (in brackets the SEE as %).

&:  $\eta$  shrinkage of empirical Bayesian estimates to the population values.

#:  $\epsilon$  shrinkage of model output to the observations

#### 4.3.3 UTILITY FUNCTION

The calculated UFs are shown in Fig. 7A and B. In the concentration domain ( $U_1$ , eqn. 3), the utility is positive for low fentanyl effect-site or steady-state concentrations ( $< 0.7$  ng.ml<sup>-1</sup>, fig. 7B). At high concentrations the function is negative indicating that the chance for respiratory depression of 50% or greater exceeds the chance for analgesia (increase in pain tolerance by 50% or more). At a concentration of 1.74 ng.ml<sup>-1</sup> the UF was most negative ( $U_1 = -0.23$ ) with a chance for analgesia and respiratory depression of 60% and 83%, respectively.

In the time domain ( $U_2$ , eqn. 4, Fig. 7A), the UF after a fentanyl dose of 3.5  $\mu$ g.kg<sup>-1</sup> is initially negative due to the high fentanyl concentrations from the bolus infusion (at  $t = 6.6$  min the value of  $U_2 = -0.44$  with changes for analgesia and respiratory depression of 21% and 65%). With decreasing concentrations the function becomes positive at  $t > 100$  min. This corresponds with plasma fentanyl concentrations  $< 0.6$  ng.ml<sup>-1</sup>. At  $t = 240$  min the value of  $U = 0.06$  with changes for analgesia and respiratory depression of 10% and 4% respectively.

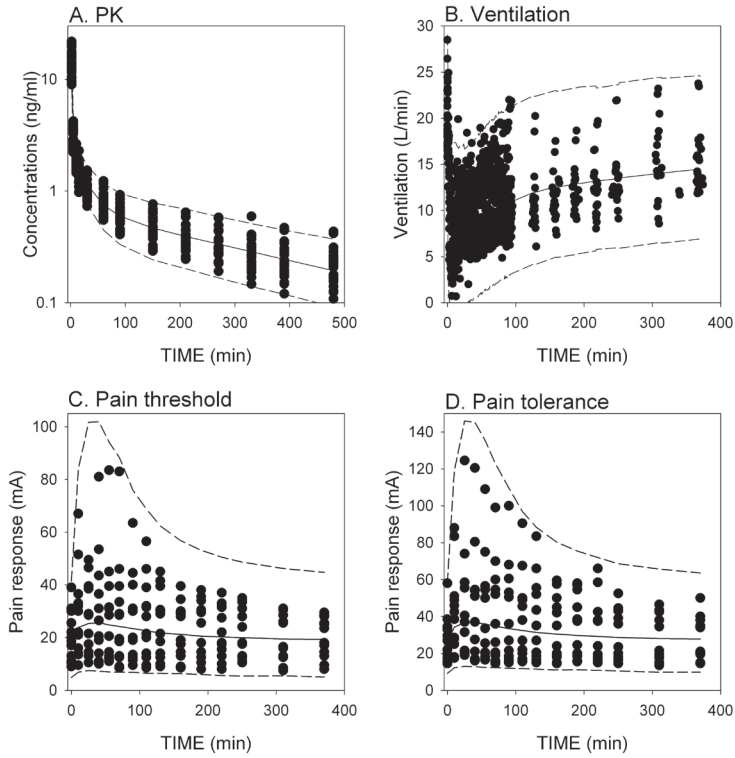


**Figure 6.** Visual Predictive Checks of the fentanyl pharmacokinetic and pharmacodynamic model outcomes. Simulations performed with an input function similar to the current study.

A. Fentanyl concentration. B. Ventilation. C. Pupil diameter. D. Pain tolerance. E. Pain threshold. Continuous lines: the median data fit; broken lines  $\pm 95\%$  confidence intervals.

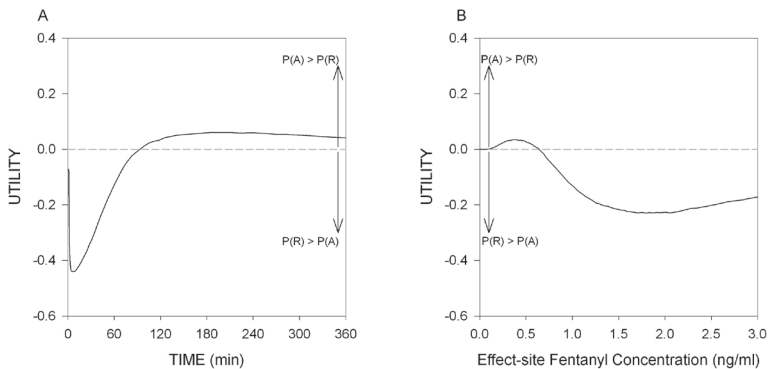


**Figure 7.** Utility functions ( $P(A \geq 50\%) - P(R \geq 50\%)$ ) for respiratory responses and pain relief in the time (A, following a  $3.5 \mu\text{g}\cdot\text{kg}^{-1}$  injection) and concentration domains (B), where  $P(A \geq 50\%)$  is the probability for an increase in pain tolerance of 50% or greater and  $P(R \geq 50\%)$  is the probability for respiratory depression of 50% or greater.  $P(A) > P(R)$  indicates that the probability for positive effects (analgesia) exceeds the probability for negative effects (respiratory depression);  $P(R) > P(A)$  indicates that the probability for negative effects (respiratory depression) exceeds the probability for positive effects (analgesia).

## 4.3.4 SENSITIVITY ANALYSIS

**Effect of variations in P(A) and P(R) response thresholds.** The results of the sensitivity analyses are given in Fig. 8A and B. Fig. 8A shows the results of the analyses in the concentration domain, while Fig. 8B gives the analyses in the time domain. Each set of lines with identical lines represents a set of fixed probabilities for respiratory depression, while within these sets the probability for analgesia increases from top to bottom. For analgesia, the probability for greater analgesic effects (for example  $P(A > 75\%)$ ) or an increase in pain tolerance of at least 75% occurs at the lower end of the set as the greater opioid concentrations that are required to reach such analgesic levels coincide with a greater probability for respiratory depression. For respiratory depression, going from  $P(R > 75\%)$  to  $P(R > 25\%)$  the probability for respiratory depression increases irrespective of the P(A) thresholds. For example, the probability of respiratory depression of at least 25%,  $P(R > 25\%)$ , exceeds that observed for the other effect threshold values, and consequently the function  $P(A) - P(R)$  is more negative than the other functions.

**Effect of variations in (pain model) parameter estimates  $t_{1/2}k_{e0}$  and  $C_{50}$ .** The results are given in figure 9 and show that an increase in analgesic potency and, although to a lesser extent, a smaller value for  $t_{1/2}k_{e0}$  causes an upward shift of the utility function. The reverse is true in case of a lesser analgesic potency and a slower analgesic onset/offset.

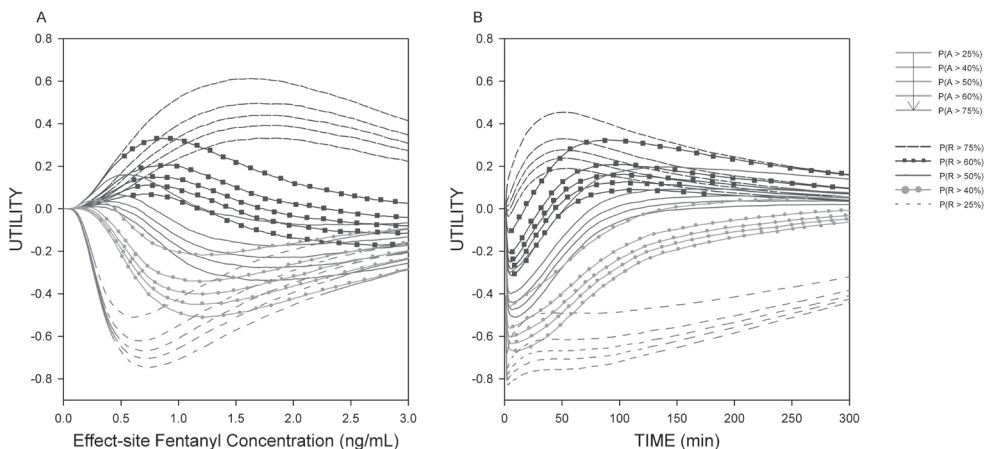


**Figure 8.** Sensitivity analysis of the effect of different numerical response thresholds in P(A) and P(R) on the shape of the utility functions. Each set of lines with identical lines represents a set of fixed probabilities for respiratory depression, while within these sets the probability for analgesia increases from top to bottom (See legend). **A.** UFs in the concentration domain. **B.** Utility functions in the time domain.

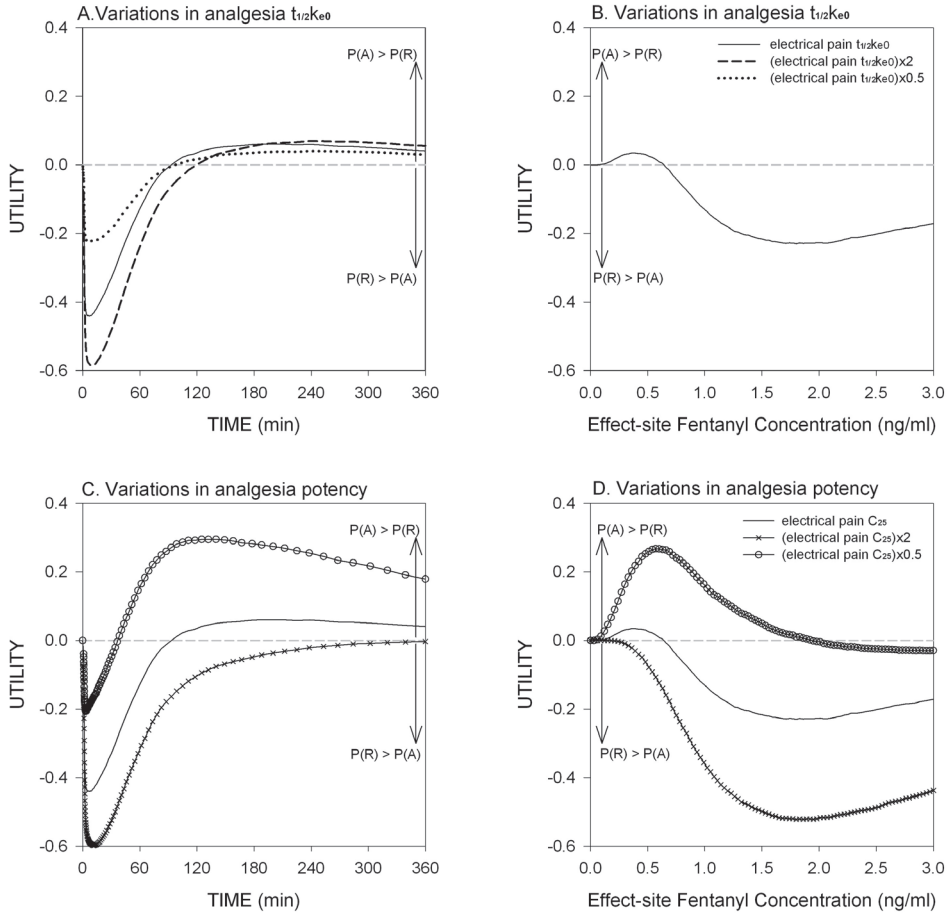


**Figure 9.** Influence of variations in blood-effect-site equilibration half-life,  $t_{1/2}k_{e0}$  (A and B), and potency parameter,  $C_{50}$  (C and D), on the shape of the utility functions (UFs). Continuous lines are the data estimated from the current study (UF in time domain are constructed for a 3.5  $\mu\text{g}/\text{kg}$  fentanyl injection). A and B. Dashed line is the UF with analgesia's  $t_{1/2}k_{e0} \times 2$ , the dotted line is the UF with analgesia's  $t_{1/2}k_{e0} \times 0.5$  (Note that in the concentration domain changes in  $t_{1/2}k_{e0}$  do not affect the shape of the UF). C and D. x-x- are the UFs with a lower potency for analgesia ( $C_{25} \times 2$ ), o-o- are the UFs with a higher potency for analgesia ( $C_{25} \times 0.5$ ).



## 4.4 DISCUSSION

The risk of opioid toxicity is best considered in the context of the opioid's benefit (*i.e.* analgesia). Integrating opioid risk and benefit is important in acute and chronic pain treatment as it allows the comparison of net efficacy among opioids. For example, Katz showed in 946 patients with chronic lower back pain that the risk-benefit composite (defined as the proportion of days where the patient is an opioid responder (*ie.* experiencing  $\geq 30\%$  pain relief) with no or just moderate adverse events) is significantly greater for the opioid tapentadol than for oxycodone (30 vs. 25%).\* This may help in the choice of opioid treatment for that specific patient population. In the current study, we assessed the risk-benefit composite of fentanyl in an acute administration paradigm by construction of a Utility Function as previously described by Cullberg,<sup>6</sup> *i.e.* the difference between the probability of a wanted effect (antinociception, a positive effect) minus the probability of a side effect (respiratory depression, a negative effect).

The UF is context sensitive. The context is the chosen probability for effect and side effect. We chose  $P(A \geq 0.5) - P(R \geq 0.5)$  which is the probability for an increase in pain tolerance of at least 50% minus the probability for 50% respiratory depression or more. We choose 50% as it compares to other 50% response values used in anesthesia such as minimum alveolar concentration (which gives the anesthetic concentration causing a response in 50% of patient) and  $C_{50}$  (which is the drug concentration causing 50% effect). Evidently other probabilities will result in UFs that deviate in shape from the current functions. A sensitivity analysis using different numerical response thresholds in  $P(A)$  and  $P(R)$  does indeed show that the UF is context sensitive (Fig. 8). The response threshold of  $P(A \geq 0.5) - P(R \geq 0.5)$  is well positioned in the middle of the observed functions and reflects the "mid"-response comparable to the minimum alveolar concentration or  $C_{50}$ . How these results may be interpreted in a clinical setting and which of the response thresholds is most appropriate requires further studies.

The UFs were constructed from  $2 \times 9,999$  simulations using the PK-PD parameter estimates. The sometimes-large variance of some parameters is therefore taken into account in the UF. We determined the utility as function of effect-site or steady-state concentration ( $U_1$ , eqn. 3) and time ( $U_2$ , eqn. 4) following a  $3.5 \mu\text{g}\cdot\text{kg}^{-1}$  fentanyl injection. Following the injection,  $U_2$  values are negative for the first 90 min with large negative values ( $< -0.4$ ) from  $t = 2$  to  $t = 17$  min (Fig. 6A). At  $t > 90$  min, when plasma fentanyl concentrations were  $< 0.6 \text{ ng}\cdot\text{mL}^{-1}$ ,  $U_2$  becomes positive, but the positive values are small. The  $U_1$  (concentration) function shows a variation of 0.25, a rather modest variation ranging from +0.05 to -0.20, but still predominantly negative (Fig. 6B). Overall the UFs show what also clinically is apparent: (1) following a fentanyl bolus dose the probability of respiratory depression (relative to analgesia) is highest in the first hour following the injection, with a diminishing (but certainly not vanishing) probability of respiratory depression at later times; and (2) only at low doses of fentanyl (up to  $50 \mu\text{g}$ ) does the probability for analgesia exceed that of respiratory depression.

The UFs we constructed are based on specific pharmacodynamic end-points commonly used in our laboratory when studying opioid effect and therefore allow comparison among opioids. Ventilation was measured with the dynamic end-tidal forcing technique in which the end-tidal PCO<sub>2</sub> is clamped at a fixed elevated level such that pre-drug baseline ventilation increased to 20 - 24 L.min<sup>-1</sup>.<sup>(7-10,15-17)</sup> This approach has various advantages including the assessment of respiratory effect at constant carbon dioxide stimulation. Under 'non-clamped' conditions (i) the arterial carbon dioxide level changes over time following the administration of an opioid resulting in confounding variations in the stimulation of peripheral and central chemoreceptors, and (ii) the speed of opioid injection influences the time profile of respiratory depression.<sup>18</sup> The estimated model parameters of the respiratory effects of fentanyl ( $C_{50} = 1 \text{ ng.ml}^{-1}$ ,  $t_{1/2k_{e0}} = 17 \text{ min}$ ) are in close agreement with earlier observations in healthy volunteers.<sup>9,19</sup> In the current study,  $C_{50}$  is the fentanyl concentration at the effect site (or the steady-state plasma concentration) causing 50% depression of ventilation under conditions of a clamped and elevated end-tidal carbon dioxide concentration. Under non-clamped conditions the estimated  $C_{50}$  value will result in an increase in arterial PCO<sub>2</sub> by 30 to 40% combined with a reduction in ventilation by 30-40%.

The nociceptive model used by us is transcutaneous electrical stimulation. This model is used frequently in pain research as it allows repetitive testing without confounders such as sensitization or adaptation.<sup>10-12,19</sup> The opioid response to electrical stimulation is slower than expected from other end-points including respiratory depression and changes in electroencephalographic parameters.<sup>11,19-22</sup> The slower response has been observed for other opioids as well and is further discussed by Olofson *et al.*,<sup>11</sup> It is most probably related to slow neuronal dynamics and activation of short-term potentiation at central sites involved in the processing of electrical pain.<sup>11</sup> Irrespective, the fentanyl potency value ( $C_{25} = 0.9 \text{ ng.mL}^{-1}$ ; extrapolated  $C_{50} = 1.4 \text{ ng.mL}^{-1}$ ) is well within the expected clinical concentration range and corresponds with the concentration causing a 40% reduction in isoflurane minimum alveolar concentration and potent analgesia in clinical settings.<sup>23</sup> To get an indication of the importance of variations in  $t_{1/2k_{e0}}$  and potency on the shape of the UFs we performed an additional set of simulations (Fig. 9) with variations in the analgesia model parameters. Variation in  $C_{25}$  was the more dominant factor with larger changes in the shape of the UF compared to changes in  $t_{1/2k_{e0}}$ . At a lower analgesic potency the UF becomes more negative, both in time and concentration domains. A smaller value for  $t_{1/2k_{e0}}$  (ie. a more rapid onset/offset of effect) results in an upward shift of the UF (Fig. 9A). Variations in  $t_{1/2k_{e0}}$  have no effect on the steady-state UF (Fig. 9B).

The UF in drug research is still experimental and our study is exploratory. It may already be argued that the UF may be useful for comparing the safety profile of specific drugs and for choosing a specific opioid dose with an optimal UF. Traditionally the behavior of opioids is presented in terms of concentration-effect relationships (Fig. 10). However, in contrast to the UF, such static relationships do not take into account the dynamics of

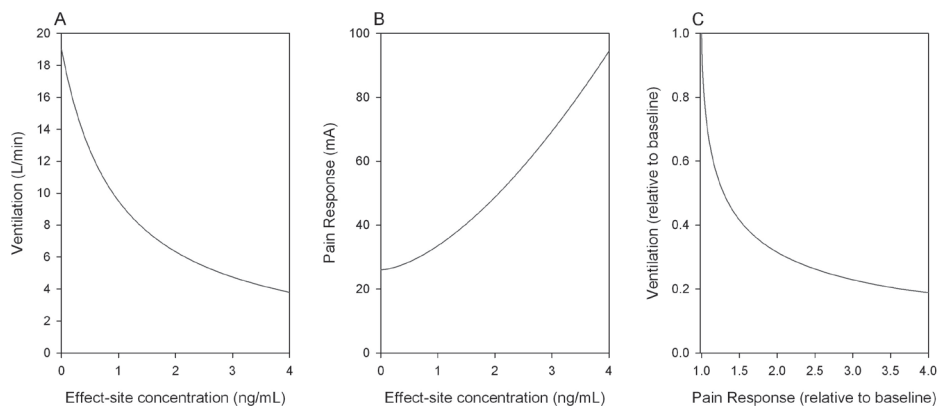


**Figure 10.** Static fentanyl concentration-effect relationships (A and B) and static pharmacodynamic-pharmacodynamic analysis (C). **A.** Fentanyl effect-site concentration versus respiratory depression. **B.** Fentanyl effect-site concentration versus pain response (pain tolerance). **C.** Ventilation versus pain response (values are aligned at identical effect-site concentration).

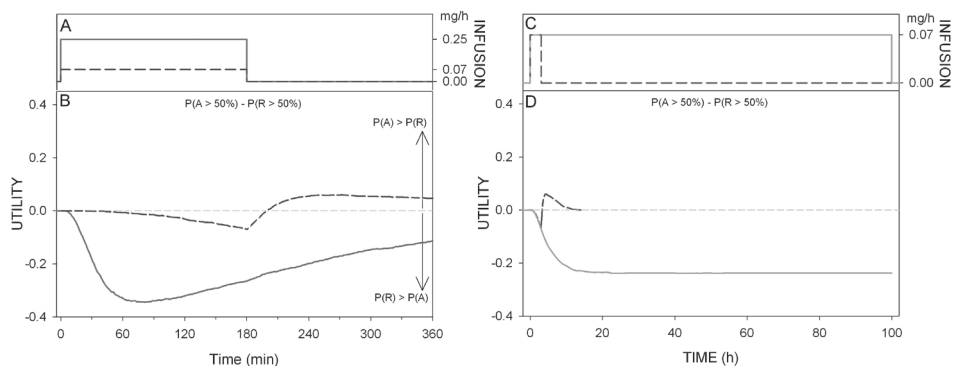


**Figure 11.** Effect of a continuous fentanyl infusion (A and C) on the utility function ( $P(A \geq 50\%) - P(R \geq 50\%)$ ) for respiratory responses and pain relief over time (B and D). **A and B.** Infusion duration is 3 h. Continuous line: fentanyl dose =  $0.25 \text{ mg}\cdot\text{h}^{-1}$  in a 70 kg patient; dashed line: fentanyl dose =  $0.07 \text{ mg}\cdot\text{h}^{-1}$  in a 70 kg patient. **C and D.** Infusion duration is 100 h (continuous line) and 3 h (dashed line).

the response (as represented in our model by parameter  $t_{1/2}k_{e0}$ ) and most importantly do not address the large inter-individual variability in the measured responses. While the static relationships are important in understanding the steady-state behavior of the opioid (for example, such analyses enable the direct comparison of multiple effects, Fig. 10C), the UF gives an insightful and dynamic presentation of possible drug effects in time and concentration domains in terms of probability of occurrence of multiple effects. For example, in Fig. 11, UFs are created for two 3-h continuous infusions of fentanyl (one at relative high dose:  $0.25 \text{ mg}\cdot\text{h}^{-1}$  for a 70 kg patient; and one at a dose commonly used

for treatment of chronic pain in transdermal patch formulations:  $0.07 \text{ mg}\cdot\text{h}^{-1}$ ) and one 100 h infusion (dose  $0.07 \text{ mg}\cdot\text{h}^{-1}$ ). As expected the UF is initially more negative for the high-dose infusion (minimum value  $-0.34$ ; Fig. 11 A and B). Subsequently this UF slowly increases due the increase in the probability for analgesia. At the low-dose infusion (Fig. 11C and D), the UF value slowly decreases in value (*i.e.* it becomes more negative over time) as the probability for respiratory depression increases more than the probability for analgesia. The UF reaches a steady state after 17-18 h (steady-state value  $-0.23$ , Fig. 11D). This suggests that patients on a fentanyl patch have a predominant (moderate) negative UF. Ending the  $0.07 \text{ mg}\cdot\text{h}^{-1}$  infusion after 3 h causes an increase in UF to a positive value (maximum value  $+0.06$ , Fig. 11B). Such behaviors could not be predicted from static concentration-effect relationships. Apart from respiratory depression other end-points may be used in the construction of UFs, including sedation, dizziness, nausea/vomiting, and psychomimetic side effects.

In conclusion, we performed an explorative study on the construction of utility functions in which the probability for respiratory depression is subtracted from the probability for analgesia as part of a risk-benefit analysis of opioid effect. The shape of the utility function is dependent on the context, that is the numerical response thresholds for P(A) and P(R) as well as the administration history (*i.e.* the change in effect-site concentration over time). In the current study probabilities for P(A) and P(R) of  $\geq 50\%$  were used that reflect an increase in pain tolerance of at least 50% and respiratory depression of at least 50%. These functions are useful in the comparison of the safety profile among drugs relative to their analgesic efficacy, and consequently may become an important tool in drug development. Further studies are required to compare our experimental data with clinical observations and assess whether the UF is valuable in clinical practice as well.

## REFERENCES

1. Dahan A, Aarts L, Smith TW. Incidence, reversal and prevention of opioid-induced respiratory depression. *Anesthesiology* 2010; 112: 226-38
2. Okie S. A flood of opioids, a rising tide of deaths. *N Eng J Med* 2010; 363: 1981-5
3. Löttsch J, Dudziak R, Freynhagen R, Marschner J, Geisslinger G: Fatal respiratory depression after multiple intravenous morphine injections. *Clin Pharmacokinet* 2006; 45: 1051-60
4. Hill LR, Pichel AC: Respiratory arrest after cadaveric renal transplant. *Eur J Anaesthesiol* 2009; 26: 435-6
5. Overdyk F, Niesters M, Dahan A. Respiratory depression: The common fatal pathway for non fatal conditions (Abstract). 2012 ASA meeting, Washington DC, Abstract 583
- Cullberg M, Eriksson UG, Wähländer K, Eriksson H, Schulman S, Karlsson MO. Pharmacokinetics of ximelagatran and relationship to clinical response in deep vein thrombosis. *Clin Pharmacol Ther* 2005; 77: 270-90
- Dahan A, DeGoede J, Berkenbosch A, Olivier ICW: The influence of oxygen on the ventilatory response to carbon dioxide in man. *J Physiol* 1990; 428: 485-99
- Dahan A, Nieuwenhuijs D, Teppema L: Plasticity of central chemoreceptors: Effect of bilateral carotid body resection on central CO<sub>2</sub> sensitivity. *PLoS Med* 2007; 4: e239

9. Yassen A, Olofsen E, Romberg R, Sarton E, Teppema L, Danhof M, Dahan A: Mechanism-based PK/PD modeling of the respiratory depressant effect of buprenorphine and fentanyl in healthy volunteers. *Clin Pharmacol Ther* 2007; 81: 50-8
10. Dahan A, Romberg R, Teppema L, Sarton E, Bijl H, Olofsen E: Simultaneous measurement and integrated analysis of analgesia and respiration after an intravenous morphine infusion. *Anesthesiology* 2004; 101: 1201-9
11. Olofsen E, Romberg R, Bijl H, Mooren R, Engbers F, Kest B, Dahan A: Alfentanil and placebo analgesia: No sex differences detected in models of experimental pain. *Anesthesiology* 2005; 103: 130-9
12. Sarton E, Olofsen E, Romberg R, den Hartigh J, Kest B, Nieuwenhuis D, Burm A, Dahan A: Sex differences in morphine analgesia: An experimental study in healthy volunteers. *Anesthesiology* 2000; 93: 1245-54
13. Beal BL, Sheiner LB, Boeckman AJ, Bauer RJ. NONMEM User's Guide. Icon development Solutions, Ellicott City, Maryland, USA. 1989-2011
14. Yassen Y, Olofsen E, Kan J, Dahan A, Danhof M: Pharmacokinetic-pharmacodynamic modeling of the effectiveness and safety of buprenorphine and fentanyl in rats. *Pharm Res* 2008; 25: 183-93
15. Choi SD, Spaulding BC, Gross JB, Apfelbaum JL: Comparison of the ventilatory effects of etomidate and methohexital. *Anesthesiology* 1985; 62: 442-7
16. Babenco HD, Conard PF, Gross JB: The pharmacodynamics effect of a remifentanyl bolus on ventilatory control. *Anesthesiology* 2000; 92: 393-8
17. Cartwright CR, Henson LC, Ward DS: Effects of alfentanil on the ventilatory response to sustained hypoxia. *Anesthesiology* 1998; 89: 612-9
18. Olofsen E, Boom M, Nieuwenhuijs D, Sarton E, Teppema L, Aarts L, Dahan A: Modeling the non-steady-state respiratory effects of remifentanyl in awake and propofol sedated healthy volunteers. *Anesthesiology*, 2010; 212: 1382-95
19. Dahan A, Yassen A, Bijl H, Romberg R, Sarton E, Teppema L, Olofsen E, Danhof M: A comparison of the respiratory effects of intravenous buprenorphine and fentanyl in humans and rats. *Br J Anaesth* 2005, 96: 825-34.
20. Coda BA, Cleveland Brown M, Risler L, Syrjala K, Shen DD: Equivalent analgesia and side effects during epidural and pharmacokinetically tailored intravenous infusion with matching plasma alfentanil concentration. *Anesthesiology* 1999; 90: 98-108.
21. Scott JC, Ponganis KV, Stanski DR: EEG quantitation of narcotic effect: The comparative pharmacodynamics of fentanyl and alfentanil. *Anesthesiology* 1985; 62: 234-41
22. Scott JC, Cooke JE, Stanski DR: Electroencephalographic quantitation of opioid effect: Comparative pharmacodynamics of fentanyl and sufentanil. *Anesthesiology* 1991; 73: 34-42
23. McEwan AI, Smith C, Dyar O, Goodman D, Smith LR, Glass PSA: Isoflurane minimum alveolar concentration reduction by fentanyl. *Anesthesiology* 1993; 78: 864-0